Utility of ^{18}F-rhPSMA-7.3 PET for Imaging of Primary Prostate Cancer and Preoperative Efficacy in N-Staging of Unfavorable Intermediate- to Very High-Risk Patients Validated by Histopathology

Thomas Langbein[1], Hui Wang[1,2], Isabel Rauscher[1], Markus Kroenke[1], Karina Knorr[1], Alexander Wurzer[3], Kristina Schwamborn[4], Tobias Maurer[5], Thomas Horn[6], Bernhard Haller[7], Hans-Jürgen Wester[3], and Matthias Eiber[1]

[1]Department of Nuclear Medicine, Klinikum Rechts der Isar, School of Medicine, Technical University of Munich, Munich, Germany; [2]Department of Nuclear Medicine, West China Hospital, Sichuan University, Chengdu, China; [3]Chair of Radiopharmacy, Technical University of Munich, Munich, Germany; [4]Institute of Pathology, Klinikum Rechts der Isar, School of Medicine, Technical University of Munich, Munich, Germany; [5]Martini-Klinik and Department of Urology, University Hospital Hamburg–Eppendorf, Hamburg, Germany; [6]Department of Urology, Klinikum Rechts der Isar, School of Medicine, Technical University of Munich, Munich, Germany; and [7]Institute of Medical Informatics, Statistics and Epidemiology, School of Medicine, Technical University of Munich, Munich, Germany

^{18}F-rhPSMA-7.3, the lead compound of a new class of radiohybrid prostate-specific membrane antigen (rhPSMA) ligand, is currently in phase III trials for prostate cancer (PCa) imaging. Here, we describe our experience in primary PCa staging. **Methods:** We retrospectively identified 279 patients with primary PCa who underwent ^{18}F-rhPSMA-7.3 PET/CT (staging cohort). A subset of patients (83/279) subsequently underwent prostatectomy with lymph node (LN) dissection without prior treatment (efficacy cohort). The distribution of tumor lesions was determined for the staging cohort and stratified by National Comprehensive Cancer Network risk score. Involvement of pelvic LNs was assessed retrospectively by 3 masked independent central readers, and a majority rule was used for analysis. Standard surgical fields were rated on a 5-point scale independently for PET and for morphologic imaging. Results were compared with histopathologic findings on a patient, right-vs.-left, and template basis. **Results:** For the staging cohort, ^{18}F-rhPSMA-7.3 PET was positive in 275 of 279 (98.6%), 106 of 279 (38.0%), 46 of 279 (16.5%), 65 of 279 (23.3%), and 5 of 279 (1.8%) patients for local, pelvic nodal, extrapelvic nodal, metastatic bone, and visceral metastatic disease, respectively. In the efficacy cohort, LN metastases were present in 24 of 83 patients (29%) and were located in 48 of 420 (11%) resected templates and in 33 of 166 (19.9%) hemipelvic templates in histopathology. The majority vote results showed that patient-level sensitivity, specificity, and accuracy for pelvic nodal metastases were 66.7% (95% CI, 44.7%–83.6%), 96.6% (95% CI, 87.3%–99.4%), and 88.0% (95% CI, 78.5%–93.8%), respectively, for ^{18}F-rhPSMA-7.3 PET and 37.5% (95% CI, 19.6%–59.2%), 91.5% (95% CI, 80.6%–96.8%), and 75.9% (95% CI, 65.0%–84.3%), respectively, for morphologic imaging. ^{18}F-rhPSMA-7.3 showed higher interobserver agreement than morphologic imaging (patient-level Fleiss $\kappa = 0.54$ [95% CI, 0.47–0.62] vs. 0.24 [95% CI, 0.17–0.31]). A mean SUV ratio of 6.6 (95% CI, 5.2–8.1) documented a high image contrast between local tumors and adjacent low urinary tracer retention. **Conclusion:** ^{18}F-rhPSMA-7.3 PET offers diagnostic performance superior to morphologic imaging for primary N-staging of newly diagnosed PCa, shows lower interreader variation, and offers good distinction between primary-tumor activity and bladder background activity. With increasing National Comprehensive Cancer Network risk group, an increasing frequency of extraprostatic tumor lesions was observed.

Key Words: ^{18}F-rhPSMA-7.3; PET; primary prostate cancer; lymph node metastases; histopathology; interobserver agreement

J Nucl Med 2022; 63:1334–1342
DOI: 10.2967/jnumed.121.263440

In recent years, prostate-specific membrane antigen (PSMA) PET with tracers such as ^{68}Ga-PSMA-11 has become increasingly used for diagnostic imaging in patients with prostate cancer (PCa) (*1*). The proPSMA trial established that ^{68}Ga-PSMA-11 PET, compared with conventional imaging, is a superior imaging modality for patients with primary high-risk PCa but histopathologic validation of the ^{68}Ga-PSMA-11 PET findings is lacking in most lesions (*2*). Most recently, a bicentric phase III trial reported the diagnostic accuracy of ^{68}Ga-PSMA-11 for pelvic N-staging (*3*). In addition to multiple mainly retrospective series, these studies were pivotal for the recent integration of PSMA-ligand PET into various guidelines and for the Food and Drug Administration approval of ^{68}Ga-PSMA-11 (*4–6*).

However, ^{68}Ga-PSMA-11 is not without disadvantages. Substantial accumulation in the urinary bladder through rapid urinary excretion can hinder detection of pelvic lesions (*7,8*). Conversely, because of the longer half-life of ^{18}F-labeled PSMA ligands, along with their potential for larger-batch production and their lower positron range resulting in higher image spatial resolution, they offer several logistical benefits and potential for better performance than their ^{68}Ga-labeled counterparts (*9*). ^{18}F-DCFPyL was recently approved by the Food and Drug Administration for biochemical recurrence, but it also exhibits high tracer retention in the urinary system (*10,11*).

Radiohybrid PSMA (rhPSMA) ligands are a new class of diagnostic and therapeutic PSMA ligands that can be efficiently labeled

Received Oct. 26, 2021; revision accepted Dec. 28, 2021.
For correspondence or reprints, contact Thomas Langbein (thomas.langbein@tum.de).
Published online Jan. 6, 2022.

with ^{18}F and with radiometals (*12*). Promising preliminary imaging data (*13,14*) have been reported for ^{18}F-rhPSMA-7, which comprises 4 diastereoisomers. One of these, ^{18}F-rhPSMA-7.3, was selected as the lead rhPSMA compound for clinical development based on preclinical data (*15*). To date, the safety and biodistribution of ^{18}F-rhPSMA-7.3 have been established in healthy volunteers and PCa patients. ^{18}F-rhPSMA-7.3 has been shown to have low average urinary excretion, and diagnostic efficacy has been demonstrated in patients with biochemical recurrence of PCa (*16–18*). ^{18}F-rhPSMA-7.3 is currently under evaluation in 2 phase III studies, for primary and biochemical recurrence of PCa (NCT04186845 and NCT04186819).

The present retrospective analysis provides the first data, to our knowledge, on use of ^{18}F-rhPSMA-7.3 PET for primary staging in patients with newly diagnosed PCa. Specifically, we aimed to describe the distribution of tumor lesions stratified by National Comprehensive Cancer Network (NCCN) risk groups (*4*) and to evaluate interobserver variability and diagnostic performance for preoperative N-staging in patients with unfavorable intermediate- to very high-risk disease.

MATERIALS AND METHODS

Study Design and Patient Populations

We retrospectively extracted data from all patients included in our institution's database who underwent ^{18}F-rhPSMA-7.3 PET/CT for primary staging of PCa between November 2018 and April 2020 (staging cohort; $n = 279$). To analyze the interobserver variability and diagnostic efficacy of ^{18}F-rhPSMA-7.3 PET for N-staging validated by histopathology, we selected all patients who underwent subsequent radical prostatectomy and extended pelvic lymph node (LN) dissection (efficacy cohort; $n = 83$). Table 1 presents patient characteristics for both groups. Figure 1 details the cohorts and outlines the clinical, imaging, and histopathologic data that were collected.

The retrospective analysis was approved by the Ethics Committee of the Technical University Munich (permit 99/19), and the requirement to obtain informed consent was waived. The administration of ^{18}F-rhPSMA-7.3 complied with the German Medicinal Products Act, AMG §13 2b, and the responsible regulatory body (Government of Oberbayern).

^{18}F-rhPSMA-7.3 Synthesis, Administration, and Image Acquisition

^{18}F-rhPSMA-7.3 was synthesized as recently reported (*12*) and administered as an intravenous bolus (median, 335 MBq; range, 301–372 MBq) a median of 72 min (range, 65–80 min) before the scan. Patients underwent ^{18}F-rhPSMA-7.3 PET/CT on a Biograph mCT Flow scanner (Siemens Medical Solutions) as recently described (*13,14*). All patients received a diagnostic CT scan after intravenous contrast injection (Iomeron 300 [Bracco], weight-adapted, 1.5 mL/kg) and oral intake of diluted contrast medium (300 mg ioxitalamate [Telebrix; Guerbet]). Furosemide (20 mg intravenously) was administered to all patients at the time of ^{18}F-rhPSMA-7.3 injection, and patients were asked to void urine before the scan. PET scans were acquired in 3-dimensional mode with an acquisition time of 2 min per bed position in flow technique (1.1 mm/s). Emission data were corrected for randoms, dead time, scatter, and attenuation and were reconstructed iteratively by an ordered-subsets expectation maximization algorithm (4 iterations, 8 subsets) followed by a postreconstruction smoothing gaussian filter (5 mm in full width at half maximum).

Image Analysis

In the staging cohort, the distribution of tumor lesions was described using the molecular imaging TNM system from the Prostate Cancer Molecular Imaging Standardized Evaluation system (*19*). The results for this cohort were taken from the clinical reads. To determine the efficacy for pelvic N-staging, dedicated rereads of the ^{18}F-rhPSMA-7.3 PET/CT datasets from the efficacy cohort were performed by 3 board-certified nuclear medicine physicians (3, 6, and 9 y of experience in PSMA-ligand PET). The readers did not know the histopathology results. In a first step, the anatomic data using the diagnostic contrast-enhanced CT dataset were analyzed by the readers. Next, after at least 4 wk, a second read of the corresponding ^{18}F-rhPSMA-7.3 scan was performed using anatomic images only to correlate an area of suggestive uptake to the corresponding LN template. Findings for both reads were reported on a template level using a 5-point Likert scale (1, tumor manifestation; 2, probably tumor manifestation, 3, equivocal, 4, probably benign, 5, benign).

To determine the contrast between local primary-tumor uptake and bladder retention of ^{18}F-rhPSMA-7.3, SUV_{mean} for ^{18}F-rhPSMA-7.3 was determined within standardized isocontour volumes of interest with 40% of the SUV_{max}, drawn over the bladder and the primary-tumor lesion.

Histopathology

Extended pelvic lymphadenectomy was performed as previously described (*20,21*) to collect right/left common iliac vessel, right/left internal iliac vessel, right/left external iliac vessel, and right/left obturator fossa standard LN templates. Further templates (e.g., presacral/pararectal) were resected if the ^{18}F-rhPSMA-7.3 PET had shown positive LNs outside these regions. The uropathologists did not know the imaging data.

Statistical Analysis

For quantitative measurements, mean values and SDs are presented. ^{18}F-rhPSMA-7.3 PET and morphologic imaging results were compared with histopathologic results from resected LNs on a patient, right-vs.-left, and template basis. Overall diagnostic accuracy was assessed using receiver-operating-characteristic (ROC) analyses. Areas under the ROC curves, with 95% CIs, were compared for both ^{18}F-rhPSMA-7.3 PET and morphologic imaging. For the patient-based analysis, the method by DeLong et al. (*22*) for 2 correlated ROC curves was used, and that by Obuchowski (*23*) was used for right-vs.-left–based and template-based analyses to account for the multiple assessments within a patient.

A dichotomization of the 5-point Likert scale ratings was performed for analysis of the sensitivity, specificity, and accuracy of the ^{18}F-rhPSMA-7.3 PET and morphologic imaging. To reflect a real-world approach, equivocal findings were counted as positive. To estimate cumulative diagnostic results from all 3 readers, a majority vote was used. The results from all 3 readers dichotomized into negative and positive assessments were compared, and in cases of any disagreement, the final assessment was based on the majority decision (i.e., a 2:1 decision).

For the patient-level analyses, exact CIs were estimated for these measures. For the right-vs.-left–based and template-based analyses, logistic generalized estimating equation models were fitted to the data to account for the correlation of multiple observations within the same patient (*24,25*). For the generalized estimating equation model, an independent correlation structure was assumed. To investigate a correlation between NCCN risk groups and frequency of extraprostatic lesions, a χ^2 test was used. A significance level of 5% was used throughout. All statistical analyses were performed using the statistical software R (*26*), with pROC (*27*) and geepack (*28*).

Interobserver agreement was evaluated using Fleiss multiple-rater κ (*29*) on a patient, right-vs.-left, and template basis, with 95% CIs reported. Interpretation of κ was based on a reproducibility classification provided by Landis and Koch (*30*). Significant differences between

TABLE 1
Characteristics of Staging and Efficacy Cohorts

Characteristic	Staging cohort	Efficacy cohort
Patients	279 (100%)	83 (29.7%)
Age (y)		
Median	70	66
Interquartile range	63–76	62–74
Prostate-specific antigen (ng/mL)*†		
Median	13.0	11
Interquartile range	7.2–26.9	7.0–17.8
ISUP grading§		
1		0 (0%)
2	46 (16.5%)	15 (18.1%)
3	61 (21.9%)	25 (30.1%)
4	65 (23.3%)	23 (27.7%)
5	85 (30.5%)	19 (22.9%)
Neoadjuvant treatment before PET/CT	16 (5.7%)	0 (0%)
NCCN risk group		
Very low	1 (0.4%)	0 (0.0%)
Low	7 (2.5%)	0 (0.0%)
Favorable intermediate	18 (6.5%)	0 (0.0%)
Unfavorable intermediate	74 (26.5%)	36 (43.4%)
High	107 (38.4%)	32 (38.6%)
Very high	72 (25.8%)	15 (18.1%)
Time between PET/CT and surgery (d)		
Median		29
Interquartile range		15–46
Pathologic T-stage		
≤pT2c		28 (33.7%)
pT3a		18 (21.7%)
≥pT3b		37 (44.6%)
Pathologic N-stage		
pN0		59 (71.1%)
pN1		24 (28.9%)
Size of largest LN metastasis per patient (mm)		
Median		8
Range		1.5–55

ISUP = International Society of Urological Pathology.
*At time of imaging.
†Unavailable for 2 patients of staging cohort.
§Unavailable for 9 patients in staging cohort and for 1 patient in efficacy cohort.
Qualitative data are number and percentage.

methods were considered present when the 95% CI were not overlapping.

RESULTS

Distribution of Tumor Lesions on ^{18}F-rhPSMA-7.3 PET

For the staging cohort based on clinical reads, ^{18}F-rhPSMA-7.3 PET was positive for local disease in 275 of 279 patients (98.6%), for pelvic LN metastases in 106 of 279 (38.0%), for extrapelvic LN metastases in 46 of 279 (16.5%), for bone metastases in 65 of 279 (23.3%), and for visceral metastases in 5 of 279 (1.8%). On a patient level, 156 patients had only disease limited to the prostate (N0M0), and 42 patients had locoregional LN metastases but no distant metastases (N1M0). In 15 patients, extrapelvic LN metastases but no other distant metastases were present (NxM1a), and 15 patients presented with local tumor and only bone metastases (N0M1b). The distribution of extrapelvic lesions stratified by

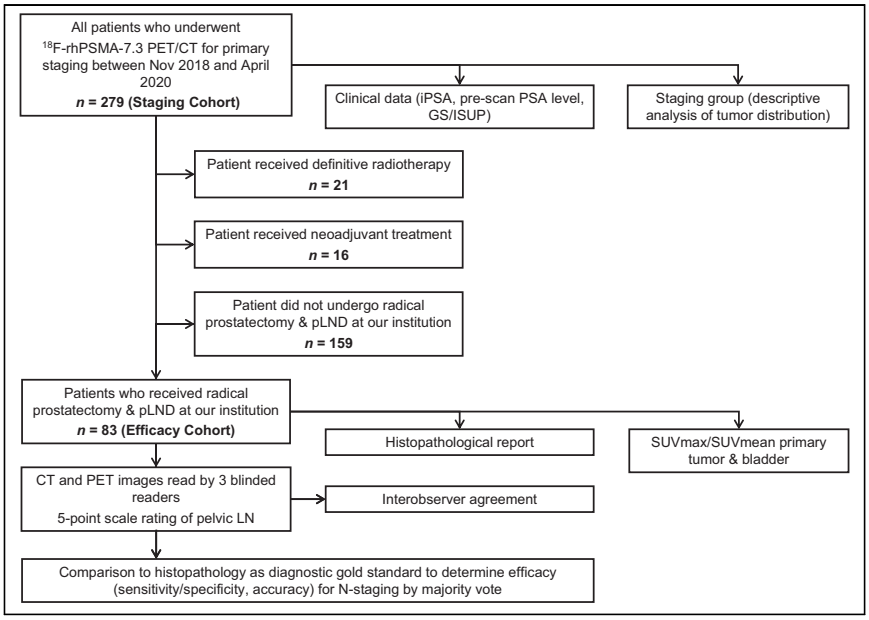

FIGURE 1. Flowchart of patient selection and data analysis. GS = Gleason score; iPSA = initial prostate-specific antigen; ISUP = International Society of Urological Pathology; pLND = pelvic LN dissection; PSA = prostate-specific antigen.

NCCN risk group is presented in Figure 2. The patient-based pattern of lesion distribution is presented in Supplemental Table 1. A moderate but highly significant correlation between risk groups and the frequency of extraprostatic lesions was found, with an increasing prevalence in higher-risk groups (Pearson χ^2 test for miN1: $\chi^2_5 = 65.6$, $P < 0.001$, $\varphi = 0.485$; for miM1: $\chi^2_5 = 31.4$, $P < 0.001$, $\varphi = 0.335$).

On the basis of clinical reads in the efficacy cohort, ^{18}F-rhPSMA-7.3 PET was positive in 82 of 83 (98.8%) and 20 of 83 (24.1%) subjects for local and pelvic nodal disease (N1M0), respectively. One and 6 patients underwent primary surgery, with distant metastases being either only extrapelvic nodal (M1a) or only metastatic bone disease (M1b), respectively. Postoperative histopathology showed LN metastases in 24 of 83 patients; the median size of the largest LN metastasis per patient was 8 mm (range, 1.5–55 mm).

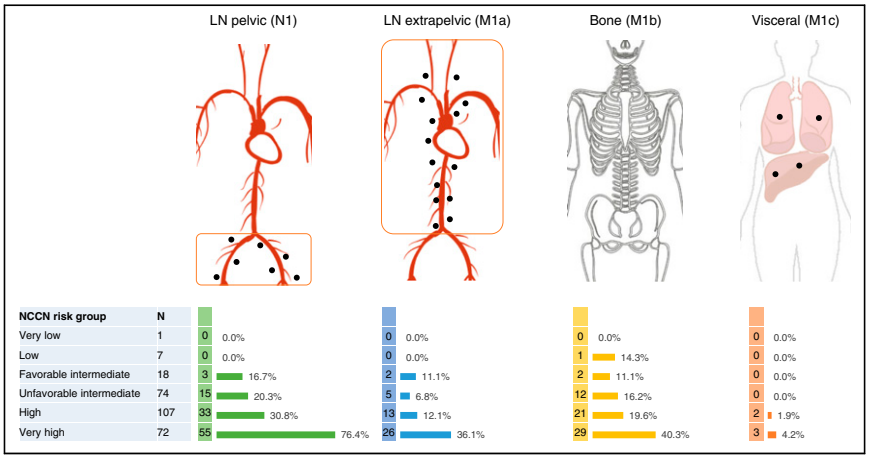

FIGURE 2. Distribution of extraprostatic tumor lesions in staging cohort (n = 279)

Diagnostic Accuracy of ^{18}F-rhPSMA-7.3 PET and Morphologic Imaging for Pelvic LN Metastases

In the efficacy cohort, LN metastases were present in 48 of 420 (11%) resected templates, in 33 of 166 (20%) hemipelvic templates, and in 24 of 83 patients (29%). In total, 1,763 nodes were removed, with a median of 20 (interquartile range, 15–27) per patient. A patient example is presented in Figure 3.

On patient-level–based majority reads, ^{18}F-rhPSMA-7.3 PET was read to be positive in 18 of 83 patients, resulting in 16 true-positive and 2 false-positive cases. It was read to be negative in 65 patients, including 8 false-negative and 57 true-negative cases. The result was a patient-level sensitivity, specificity, and accuracy for pelvic nodal metastases of 66.7% (95% CI, 44.7%–83.6%), 96.6% (95% CI, 87.3%–99.4%), and 88.0% (95% CI, 78.5%–93.8%), respectively. Morphologic imaging was read to be positive in 14 of 83 patients, resulting in 9 true-positive and 5 false-positive cases. It was read to be negative in 69 patients, including 15 false-negative and 54 true-negative cases. The corresponding patient-level sensitivity, specificity, and accuracy were 37.5% (95% CI, 19.6%–59.2%), 91.5% (95% CI, 80.6%–96.8%), and 75.9% (95% CI, 65.0%–84.3%), respectively.

On hemipelvic-based majority reads, ^{18}F-rhPSMA-7.3 PET was read to be positive in 25 of 166 assessments, resulting in 23 true-positive and 2 false-positive assessments. It was read to be negative in 141 assessments, including 10 false-negative and 131 true-negative assessments. The result was a sensitivity, specificity, and accuracy for pelvic nodal metastases of 69.7% (95% CI, 50.0%–84.1%), 98.5% (95% CI, 94.3%–99.6%), and 92.8% (95% CI, 87.4%–96.0%), respectively. Morphologic imaging was read to be positive in 15 of 166 assessments, resulting in 9 true-positive and 6 false-positive assessments. It was read to be negative in 151 assessments, including 24 false-negative and 127 true-negative assessments. The corresponding sensitivity, specificity, and accuracy were 27.3% (95% CI, 16.5%–41.6%), 95.5% (95% CI, 89.3%–98.2%), and 81.9% (95% CI, 74.9%–87.3%), respectively.

On template-based majority reads, ^{18}F-rhPSMA-7.3 PET had a sensitivity, specificity, and accuracy for pelvic nodal metastases of 70.8% (95% CI, 55.6%–82.5%), 98.3% (95% CI, 96.6%–99.2%), and 95.5% (95% CI, 93.1%–97.1%), respectively. Morphologic imaging showed a template-level sensitivity, specificity, and accuracy of 12.5% (95% CI, 6.0%–24.3%), 98.3% (95% CI, 96.6%–99.2%), and 89.5% (95% CI, 83.9%–93.4%), respectively. Detailed results for individual readers are provided in Table 2.

The ROC analysis showed a higher diagnostic performance for ^{18}F-rhPSMA-7.3 than for morphologic imaging for all 3 readers on both a patient basis and a hemipelvic

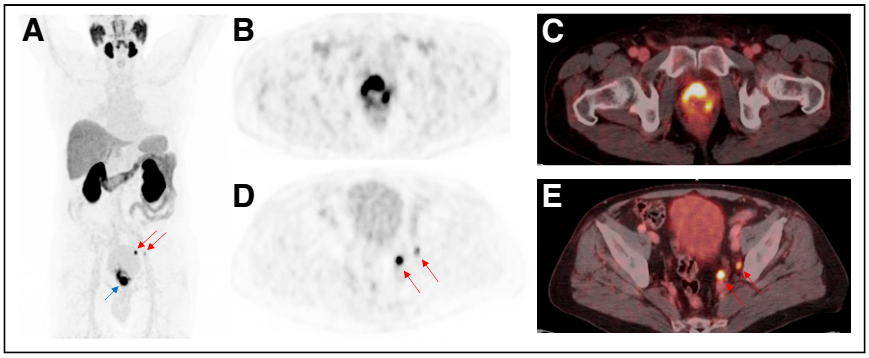

FIGURE 3. A 72-y-old patient with high-risk PCa (iPSA, 44 ng/mL) who underwent ^{18}F-rhPSMA-7.3 PET/CT illustrating primary tumor (blue arrow) and pelvic LN metastases (red arrows) histologically confirmed by radical prostatectomy (pT3b pN1 [2/34]; Gleason score, 3 + 4 = 7b): maximum-intensity projection (A); PET (B and D); fused PET/CT (C and E).

basis. On the patient-level analysis, the differences in the areas under the ROC curves were statistically significant for readers 1 and 2 on a patient basis and for all readers on a hemipelvic and template basis (Table 3).

Interobserver Agreement for Pelvic N-Staging

Interobserver agreement was significantly higher for ^{18}F-rhPSMA-7.3 PET than for morphologic imaging for assessment on a patient basis, on a hemipelvic basis, and per LN template. The patient-level interobserver agreement was moderate (Fleiss $\kappa = 0.54$; 95% CI, 0.47–0.62) for ^{18}F-rhPSMA-7.3 PET versus fair (Fleiss $\kappa = 0.24$; 95% CI, 0.17–0.31) for morphologic imaging. Similarly, interobserver agreement was moderate for left-sided nodes (Fleiss $\kappa = 0.58$; 95% CI, 0.50–0.66) and right-sided nodes (Fleiss $\kappa = 0.57$; 95% CI, 0.49–0.65) in ^{18}F-rhPSMA-7.3 PET but was only fair for left-sided nodes (left: Fleiss $\kappa = 0.20$ [95% CI, 0.12–0.27]; right: Fleiss $\kappa = 0.24$ [95% CI, 0.17–0.32]) in morphologic imaging. Supplemental Figure 1 displays the interobserver agreements and data for template-based assessments.

Uptake in Primary Tumor and Tracer Retention in Urinary Tract

^{18}F-rhPSMA-7.3 uptake in the prostate was present in 82 of 83 patients who underwent surgery, with a mean SUV_{mean} of 13.0 (range, 2.0–54.4). Retention in the urinary bladder at the time of imaging was rather low, with a mean SUV_{mean} of 2.5 (range, 0.9–18.5). Consequently, tumor-to-bladder contrast was high, with a mean ratio of 6.6 (range, 0.8–40.1) for SUV_{mean}. Data are presented in Table 4 and Supplemental Figure 2.

DISCUSSION

Here, we present a retrospective analysis on the use of ^{18}F-rhPSMA-7.3 PET/CT for primary staging of newly diagnosed PCa. The distribution of pelvic LN metastases and extrapelvic tumor lesions in this cohort was clearly associated with NCCN risk groups. In a subset of patients, we determined a high diagnostic performance of ^{18}F-rhPSMA-7.3 PET for N-staging of patients with unfavorable intermediate- to very high-risk PCa, validated by histopathology. Interobserver agreement of ^{18}F-rhPSMA-7.3 PET for N-staging among 3 independent readers showed sufficient consistency.

Currently, the standard of care for N-staging PCa relies on cross-sectional imaging and bone scintigraphy mainly in high-risk PCa (*4*). The reliable detection of LN metastases is especially challenging given the presence of LN metastases in morphologically nonenlarged LNs (*31*). Therefore, detection efficacy is low and based mainly on size, with known limitations, especially for LNs under 8 mm (*32,33*).

The clinical introduction of PSMA-targeting PET tracers offers a high potential to increase detection of LN metastases, and several studies have shown promising results with ^{68}Ga-labeled compounds (*34,35*). A prospective, multicenter study compared the accuracy of ^{68}Ga-PSMA-11 PET/CT and conventional imaging with CT and bone scanning for primary staging of pelvic LN metastases and distant metastases (*2*). The accuracy of ^{68}Ga-PSMA-11 PET/CT was superior to that of conventional imaging (92% vs. 65%), and only 15% of patients had a change of clinical management after conventional imaging, compared with 28% after ^{68}Ga-PSMA-11 PET/CT. However, the study lacked histopathologic validation of LN involvement in a substantial number of patients (only 83/302 patients underwent pelvic LN sampling). Maurer et al. conducted an early retrospective study of ^{68}Ga-PSMA-11 PET for LN staging in 130 patients with intermediate- to high-risk PCa and reported a 65.9% and 68.3% sensitivity, and a 98.9% and 99.1% specificity, on patient- and template-based analyses, respectively (*36*).

Similar specificity but lower sensitivity was reported by Klingenberg et al. in a larger retrospective investigation of newly diagnosed patients with high-risk PCa (*37*). For ^{68}Ga-PSMA-11, they reported a sensitivity, specificity, and accuracy of 30.6%, 96.5%, and 83.1%, respectively. For ^{68}Ga-PSMA-I&T in 40 patients with intermediate- or high-risk disease, Cytawa et al. found a per-region sensitivity, specificity, and accuracy of 35.0%, 98.4%, and 93.0%, respectively, for nodal metastasis detection (*38*).

Data for the recently approved ^{18}F-DCFPyL from the OSPREY trial, which investigated the detection performance for pelvic LN metastases in men with high-risk PCa, showed a specificity ranging from 96% to 99% across 3 readers, whereas sensitivity ranged from 31% to 42% (*11*). Similar to data reported for all other PSMA ligands, the specificity of ^{18}F-rhPSMA-7.3 for pelvic LN metastases is high.

The sensitivity of ^{18}F-rhPSMA-7.3 in this study (e.g., 66.7% on a patient level) appears substantially higher than that indicated by the above-mentioned data for ^{68}Ga-PSMA or ^{18}F-DCFPyL. A possible reason might be the nodal lesion size. In the efficacy cohort of our study, the median size of the largest LN metastasis per patient was 8 mm. Hope et al. demonstrated a higher sensitivity of ^{68}Ga-PSMA-11 PET in larger pelvic LN metastasis (>10 mm) (*3*). Comparable findings were shown by the OSPREY trial, where the sensitivity of ^{18}F-DCFPyL was clearly dependent on lesion size. Exclusion of lesions smaller than 5 mm resulted in a sensitivity of 60.0% (*11*). Potential other factors might also include scanner technique and reader experience.

Our retrospective analysis of the novel PSMA ligand ^{18}F-rhPSMA-7.3 confirms superiority of PSMA-targeted molecular imaging over conventional imaging for N-staging in patients with intermediate- to very high-risk primary PCa. ^{18}F-rhPSMA-7.3 achieved an overall accuracy of 88.0%, 92.8%, and 95.5% for the patient-level, hemipelvic-level, and template analyses, respectively, compared with 75.9%, 81.9%, and 89.5%, respectively, for conventional imaging.

TABLE 2
Histologically Verified Diagnostic Accuracy of ^{18}F-rhPSMA-7.3 PET and Morphologic Imaging for Preoperative N-Staging

		^{18}F-rhPSMA-7.3 PET/CT			Morphologic imaging		
Base	Reader	Sensitivity	Specificity	Accuracy	Sensitivity	Specificity	Accuracy
Patient	1	66.7% (44.7%–84.4%)	94.9% (85.9%–98.9%)	86.7% (77.5%–93.2%)	29.2% (12.6%–51.1%)	94.9% (85.9%–98.9%)	75.9% (65.3%–84.6%)
	2	70.8% (48.9%–87.4%)	96.6% (88.3%–99.6%)	89.2% (80.4%–94.9%)	41.7% (22.1%–63.4%)	89.8% (79.2%–96.2%)	75.9% (65.3%–84.6%)
	3	66.7% (44.7%–84.4%)	94.9% (85.9%–98.9%)	86.7% (77.5%–93.2%)	58.3% (36.6%–77.9%)	84.7% (73.0%–92.8%)	77.1% (66.6%–85.6%)
	Majority vote	66.7% (44.7%–83.6%)	96.6% (87.3%–99.4%)	88.0% (78.5%–93.8%)	37.5% (19.6%–59.2%)	91.5% (80.6%–96.8%)	75.9% (65.0%–84.3%)
Right vs. left	1	69.7% (50.0%–84.1%)	97.7% (93.3%–99.3%)	92.2% (86.7%–95.5%)	21.1% (11.1%–36.6%)	97.7% (93.3%–99.3%)	82.5% (75.3%–88.0%)
	2	69.7% (50.0%–84.1%)	97.0% (90.5%–99.1%)	91.6% (85.1%–95.4%)	30.3% (19.4%–43.9%)	94.0% (86.8%–97.4%)	81.3% (74.3%–86.7%)
	3	69.7% (50.0%–84.1%)	97.0% (90.6%–99.1%)	91.6% (85.6%–95.2%)	42.4% (28.4%–57.8%)	90.2% (83.5%–94.4%)	80.7% (73.8%–86.2%)
	Majority vote	69.7% (50.0%–84.1%)	98.5% (94.3%–99.6%)	92.8% (87.4%–96.0%)	27.3% (16.5%–41.6%)	95.5% (89.3%–98.2%)	81.9% (74.9%–87.3%)
Template	1	62.5% (48.5%–74.7%)	97.6% (95.5%–98.8%)	94.0% (91.0%–96.1%)	10.4% (4.5%–22.2%)	99.0% (97.5%–99.6%)	90.0% (84.2%–93.8%)
	2	64.6% (50.3%–76.6%)	97.6% (95.2%–98.8%)	94.2% (91.2%–96.2%)	18.7% (11.9%–28.4%)	97.9% (95.5%–99.0%)	89.7% (84.7%–93.3%)
	3	70.8% (55.6%–82.5%)	97.6% (95.0%–98.9%)	94.9% (92.1%–96.7%)	18.7% (8.8%–35.7%)	96.9% (94.9%–98.1%)	88.9% (83.2%–92.8%)
	Majority vote	70.8% (55.6%–82.5%)	98.3% (96.6%–99.2%)	95.5% (93.1%–97.1%)	12.5% (6.0%–24.3%)	98.3% (96.6%–99.2%)	89.5% (83.9%–93.4%)

Data in parentheses are 95% CI.

TABLE 3
DeLong Test for Correlated ROC

Basis	Reader	AUC		*P*
		^{18}F-rhPSMA-7.3 PET/CT	Morphologic imaging	
Patient	1	0.821 (0.716–0.926)	0.724 (0.606–0.843)	0.09774
	2	0.850 (0.738–0.963)	0.672 (0.526–0.817)	0.01226
	3	0.829 (0.720–0.939)	0.779 (0.662–0.896)	0.2785
Right vs. left	1	0.841 (0.745–0.938)	0.699 (0.597–0.800)	0.01195
	2	0.853 (0.762–0.944)	0.657 (0.557–0.757)	0.00041
	3	0.817 (0.708–0.925)	0.699 (0.602–0.795)	0.02655
Template	1	0.796 (0.726–0.865)	0.645 (0.579–0.712)	$6.879e^{-05}$
	2	0.822 (0.759–0.885)	0.652 (0.568–0.736)	0.00045
	3	0.847 (0.772–0.922)	0.630 (0.551–0.710)	$1.062e^{-07}$

AUC = area under ROC curve.
Data in parentheses are 95% CI.

As expected in clinical routine, we observed a clear tendency toward more frequent pelvic and extrapelvic tumor lesions with increasing NCCN group. Comparable findings have been described for the correlation of increasing prostate-specific antigen (PSA) values and the occurrence of bone metastases on bone scintigraphy for PCa staging (*39*). For example, the prevalence of bone metastases was only 2.3% at a PSA of less than 10 ng/mL, 6% at a PSA of more than 10 but less than 19.9 ng/mL, and 74.9% at a PSA of more than 100 ng/mL. For PSMA-ligand PET, the mentioned association should be considered crucial, especially in the context of primary N-staging, as nodal involvement in particular can be detected much earlier now, with a high potential to impact clinical management.

^{18}F-rhPSMA-7.3 is a single diastereoisomer of ^{18}F-rhPSMA-7, for which diagnostic accuracy has been well reported. Kroenke et al. reported the patient-level sensitivity, specificity, and accuracy of ^{18}F-rhPSMA-7 PET to be 72.2%, 92.5%, and 86.2%, respectively (*14*), which are comparable to the data in the present study. This finding supports earlier data that indicate ^{18}F-rhPSMA-7 and ^{18}F-rhPSMA-7.3 to have similar diagnostic performance for restaging patients with biochemical recurrence after radical prostatectomy (*13,18*).

A particular strength of our retrospective analysis was the evaluation of imaging data by 3 independent readers, allowing us to conduct an interobserver comparison to determine the reproducibility of interpretation of ^{18}F-rhPSMA-7.3 PET compared with morphologic imaging. The data show that the variability between ^{18}F-rhPSMA-7.3 PET readings is lower than for CT and thus suggests a more consistent, reader-independent diagnostic performance. Similar high interobserver agreement has been reported for ^{68}Ga-PSMA-11 (*40*).

A well-documented limitation of PSMA-targeting radiotracers such as ^{68}Ga-PSMA-11 and ^{18}F-DCFPyL is high retention in the urinary system and especially high accumulation in the bladder (*7,8*). For rhPSMA ligands, low retention in the urinary bladder has been reported (*41*). Our analyses for ^{18}F-rhPSMA-7.3 also revealed low urinary retention and high uptake of tumor lesions, resulting in a favorable tumor-to-bladder ratio (mean, 6.6). This could potentially increase the detection of local tumor deposits, especially in the prostate base.

Our analysis has several limitations. First, it was conducted retrospectively on a limited number of patients. This approach could—especially for the efficacy cohort—lead to a selection bias given that the cohort of patients who underwent surgery was dependent on clinical parameters, imaging results, and the patient's general health and preference. Second, the template-based analysis was limited in that the mapping between a certain LN territory in images and the surgical field is prone to errors. Third, histopathologic assessment of distant metastases was not available for most patients. ^{18}F-labeled PSMA ligands such as ^{18}F-rhPSMA-7 and ^{18}F-PSMA-1007 have been reported to exhibit a higher number of non–PCa-related uptake than ^{68}Ga-PSMA-11 (*42–45*). However, adequate reader training, interpretation in consensus with cross-sectional imaging, and the clinical context allow differentiation between

TABLE 4
^{18}F-rhPSMA-7.3 SUV_{max} and SUV_{mean} for Primary Tumors and Urinary Bladder

Parameter	Primary tumor (n = 82)		Urinary bladder (n = 82)		Primary tumor/urinary bladder (n = 82)	
	SUV_{max}	SUV_{mean}	SUV_{max}	SUV_{mean}	SUV_{max} ratio	SUV_{mean} ratio
Mean	22.4	13.0	4.3	2.5	6.6	6.6
95% CI	18.3–26.4	10.5–15.65	3.5–5.1	2.0–3.0	5.2–8.0	5.2–8.1
Range	3.6–86.9	2.0–54.4	1.6–31.4	0.9–18.5	0.8–34.2	0.8–40.1

benign uptake and disease. Fourth, our patient cohort was not exclusively patients with unfavorable intermediate- to high-risk disease. Given the local preference and, rarely, strong patient request, a few patients in lower NCCN groups underwent ^{18}F-rhPSMA-7.3 for N-staging—typical of a real-world setting.

CONCLUSION

The present study provided real-world clinical evidence that ^{18}F-rhPSMA-7.3 has moderate-to-high sensitivity and specificity for the detection of LN metastases in patients with intermediate- to very high-risk PCa. The data further showed that ^{18}F-rhPSMA-7.3 is a more reliable tool than morphologic imaging, with lower variability in image interpretation. A distinct association of nodal and extrapelvic tumor involvement with NCCN risk groups was found. ^{18}F-rhPSMA-7.3 compares well with other PSMA ligands and shows potential for good differentiation between primary-tumor uptake and background bladder retention.

DISCLOSURE

A patent application has been filed for rhPSMA (Hans-Jürgen Wester, Alexander Wurzer, and Matthias Eiber). Hans-Jürgen Wester and Matthias Eiber received funding from Blue Earth Diagnostics Ltd., Oxford, U.K. (licensee for rhPSMA), as part of an academic collaboration. Hans-Jürgen Wester is a founder, shareholder, and advisory board member of Scintomics GmbH, Fuerstenfeldbruck, Germany. Matthias Eiber reports prior consulting activities for Blue Earth Diagnostics Ltd., Novartis, Telix, Progenics, Bayer, Point Biopharma, and Janssen. No other potential conflict of interest relevant to this article was reported.

ACKNOWLEDGMENTS

Editorial support was provided by Dr. Catriona Turnbull (Blue Earth Diagnostics Ltd.). We thank Hannah Wörther for her contribution to the data collection.

KEY POINTS

QUESTION: What is the diagnostic efficacy of ^{18}F-rhPSMA-7.3 for N-staging of patients with intermediate- to very high-risk PCa in the primary setting?

PERTINENT FINDINGS: Compared with morphologic imaging, ^{18}F-rhPSMA-7.3 PET provides superior N-staging of high-risk primary PCa. The efficacy of ^{18}F-rhPSMA-7.3 compares well with published data for other PSMA ligands and offers a good tumor-to-bladder uptake ratio.

IMPLICATIONS FOR PATIENT CARE: ^{18}F-rhPSMA-7.3 PET can significantly improve primary N-staging versus conventional imaging.

REFERENCES

1. Lawhn-Heath C, Salavati A, Behr SC, et al. Prostate-specific membrane antigen PET in prostate cancer. *Radiology.* 2021;299:248–260.
2. Hofman MS, Lawrentschuk N, Francis RJ, et al. Prostate-specific membrane antigen PET-CT in patients with high-risk prostate cancer before curative-intent surgery or radiotherapy (proPSMA): a prospective, randomised, multicentre study. *Lancet.* 2020;395:1208–1216.
3. Hope TA, Eiber M, Armstrong WR, et al. Diagnostic accuracy of ^{68}Ga-PSMA-11 PET for pelvic nodal metastasis detection prior to radical prostatectomy and pelvic lymph node dissection: a multicenter prospective phase 3 imaging trial. *JAMA Oncol.* 2021;7:1635–1642.
4. NCCN clinical practice guidelines in oncology (NCCN Guidelines®): prostate cancer. NCCN website. https://www.nccn.org/professionals/physician_gls/pdf/prostate.pdf. Published May 10, 2021. Accessed June 14, 2022.
5. S3-leitlinie prostatakarzinom. Leitlinienprogramm Onkologie website. https://www.leitlinienprogramm-onkologie.de/fileadmin/user_upload/Downloads/Leitlinien/Prostatatkarzinom/Version_6/LL_Prostatakarzinom_Langversion_6.1.pdf. Published July 2021. Accessed June 14, 2022.
6. FDA approves first PSMA-targeted PET imaging drug for men with prostate cancer. FDA website. https://www.fda.gov/news-events/press-announcements/fda-approves-first-psma-targeted-pet-imaging-drug-men-prostate-cancer. Published December 1, 2020. Accessed June 14, 2022.
7. Fendler WP, Eiber M, Beheshti M, et al. ^{68}Ga-PSMA PET/CT: joint EANM and SNMMI procedure guideline for prostate cancer imaging—version 1.0. *Eur J Nucl Med Mol Imaging.* 2017;44:1014–1024.
8. Heußer T, Mann P, Rank CM, et al. Investigation of the halo-artifact in ^{68}Ga-PSMA-11-PET/MRI. *PLoS One.* 2017;12:e0183329.
9. Werner RA, Derlin T, Lapa C, et al. ^{18}F-labeled, PSMA-targeted radiotracers: leveraging the advantages of radiofluorination for prostate cancer molecular imaging. *Theranostics.* 2020;10:1–16.
10. FDA approves second PSMA-targeted PET imaging drug for men with prostate cancer. FDA website. https://www.fda.gov/drugs/drug-safety-and-availability/fda-approves-second-psma-targeted-pet-imaging-drug-men-prostate-cancer. Updated May 27, 2021. Accessed June 14, 2022.
11. Pienta KJ, Gorin MA, Rowe SP, et al. A phase 2/3 prospective multicenter study of the diagnostic accuracy of prostate specific membrane antigen PET/CT with ^{18}F-DCFPyL in prostate cancer patients (OSPREY). *J Urol.* 2021;206:52–61.
12. Wurzer A, Di Carlo D, Schmidt A, et al. Radiohybrid ligands: a novel tracer concept exemplified by 18F- or 68Ga-labeled rhPSMA inhibitors. *J Nucl Med.* 2020;61:735–742.
13. Eiber M, Kroenke M, Wurzer A, et al. 18F-rhPSMA-7 PET for the detection of biochemical recurrence of prostate cancer after radical prostatectomy. *J Nucl Med.* 2020;61:696–701.
14. Kroenke M, Wurzer A, Schwamborn K, et al. Histologically-confirmed diagnostic efficacy of ^{18}F-rhPSMA-7 positron emission tomography for N-staging of patients with primary high risk prostate cancer. *J Nucl Med.* 2019;61:710–715.
15. Wurzer A, Parzinger M, Konrad M, et al. Preclinical comparison of four [^{18}F, nat-Ga]rhPSMA-7 isomers: influence of the stereoconfiguration on pharmacokinetics. *EJNMMI Res.* 2020;10:149.
16. Tolvanen T, Kalliokoski KK, Malaspina S, et al. Safety, biodistribution and radiation dosimetry of ^{18}F-rhPSMA-7.3 in healthy adult volunteers. *J Nucl Med.* 2021;62:679–684.
17. Malaspina S, Oikonen V, Kuisma A, et al. Kinetic analysis and optimisation of ^{18}F-rhPSMA-7.3 PET imaging of prostate cancer. *Eur J Nucl Med Mol Imaging.* 2021;48:3723–3731.
18. Rauscher I, Karimzadeh A, Schiller K, et al. Detection efficacy of ^{18}F-rhPSMA-7.3 PET/CT and impact on patient management in patients with biochemical recurrence of prostate cancer after radical prostatectomy and prior to potential salvage treatment. *J Nucl Med.* 2021;62:1719–1726.
19. Eiber M, Herrmann K, Calais J, et al. Prostate cancer molecular imaging standardized evaluation (PROMISE): proposed miTNM classification for the interpretation of PSMA-ligand PET/CT. *J Nucl Med.* 2018;59:469–478.
20. Heck MM, Retz M, Bandur M, et al. Topography of lymph node metastases in prostate cancer patients undergoing radical prostatectomy and extended lymphadenectomy: results of a combined molecular and histopathologic mapping study. *Eur Urol.* 2014;66:222–229.
21. Maurer T, Souvatzoglou M, Kubler H, et al. Diagnostic efficacy of [^{11}C]choline positron emission tomography/computed tomography compared with conventional computed tomography in lymph node staging of patients with bladder cancer prior to radical cystectomy. *Eur Urol.* 2012;61:1031–1038.
22. DeLong ER, DeLong DM, Clarke-Pearson DL. Comparing the areas under two or more correlated receiver operating characteristic curves: a nonparametric approach. *Biometrics.* 1988;44:837–845.
23. Obuchowski NA. Nonparametric analysis of clustered ROC curve data. *Biometrics.* 1997;53:567–578.
24. Smith PJ, Hadgu A. Sensitivity and specificity for correlated observations. *Stat Med.* 1992;11:1503–1509.
25. Zeger SL, Liang KY. Longitudinal data analysis for discrete and continuous outcomes. *Biometrics.* 1986;42:121–130.
26. The R project for statistical computing. R Project website https://www.R-project.org/. Accessed June 14, 2022.

27. Robin X, Turck N, Hainard A, et al. pROC: an open-source package for R and S+ to analyze and compare ROC curves. *BMC Bioinformatics.* 2011;12:77.
28. Højsgaard S, Halekoh U, Yan J. The R package geepack for generalized estimating equations. *J Stat Softw.* 2005;15:1–11.
29. Hale CA, Fleiss JL. Interval estimation under two study designs for kappa with binary classifications. *Biometrics.* 1993;49:523–534.
30. Landis JR, Koch GG. The measurement of observer agreement for categorical data. *Biometrics.* 1977;33:159–174.
31. Heesakkers RA, Hovels AM, Jager GJ, et al. MRI with a lymph-node-specific contrast agent as an alternative to CT scan and lymph-node dissection in patients with prostate cancer: a prospective multicohort study. *Lancet Oncol.* 2008;9:850–856.
32. Hövels AM, Heesakkers RA, Adang EM, et al. The diagnostic accuracy of CT and MRI in the staging of pelvic lymph nodes in patients with prostate cancer: a meta-analysis. *Clin Radiol.* 2008;63:387–395.
33. Prostate cancer. EAU website. http://uroweb.org/guideline/prostate-cancer/. Accessed June 14, 2022.
34. von Eyben FE, Picchio M, von Eyben R, Rhee H, Bauman G. ^{68}Ga-labeled prostate-specific membrane antigen ligand positron emission tomography/computed tomography for prostate cancer: a systematic review and meta-analysis. *Eur Urol Focus.* 2018;4:686–693.
35. Petersen LJ, Zacho HD. PSMA PET for primary lymph node staging of intermediate and high-risk prostate cancer: an expedited systematic review. *Cancer Imaging.* 2020;20:10.
36. Maurer T, Gschwend JE, Rauscher I, et al. Diagnostic efficacy of ^{68}gallium-PSMA positron emission tomography compared to conventional imaging for lymph node staging of 130 consecutive patients with intermediate to high risk prostate cancer. *J Urol.* 2016;195:1436–1443.
37. Klingenberg S, Jochumsen MR, Ulhoi BP, et al. ^{68}Ga-PSMA PET/CT for primary lymph node and distant metastasis NM staging of high-risk prostate cancer. *J Nucl Med.* 2021;62:214–220.
38. Cytawa W, Seitz AK, Kircher S, et al. ^{68}Ga-PSMA I&T PET/CT for primary staging of prostate cancer. *Eur J Nucl Med Mol Imaging.* 2020;47:168–177.
39. Abuzallouf S, Dayes I, Lukka H. Baseline staging of newly diagnosed prostate cancer: a summary of the literature. *J Urol.* 2004;171:2122–2127.
40. Fendler WP, Calais J, Allen-Auerbach M, et al. ^{68}Ga-PSMA-11 PET/CT interobserver agreement for prostate cancer assessments: an international multicenter prospective study. *J Nucl Med.* 2017;58:1617–1623.
41. Oh SW, Wurzer A, Teoh EJ, et al. Quantitative and qualitative analyses of biodistribution and PET image quality of a novel radiohybrid PSMA, ^{18}F-rhPSMA-7, in patients with prostate cancer. *J Nucl Med.* 2020;61:702–709.
42. Grünig H, Maurer A, Thali Y, et al. Focal unspecific bone uptake on [^{18}F]-PSMA-1007 PET: a multicenter retrospective evaluation of the distribution, frequency, and quantitative parameters of a potential pitfall in prostate cancer imaging. *Eur J Nucl Med Mol Imaging.* 2021;48:4483–4494.
43. Arnfield EG, Thomas PA, Roberts MJ, et al. Clinical insignificance of [^{18}F]PSMA-1007 avid non-specific bone lesions: a retrospective evaluation. *Eur J Nucl Med Mol Imaging.* 2021;48:4495–4507.
44. Kroenke M, Mirzoyan L, Horn T, et al. Matched-pair comparison of ^{68}Ga-PSMA-11 and ^{18}F-rhPSMA-7 PET/CT in patients with primary and biochemical recurrence of prostate cancer: frequency of non-tumor-related uptake and tumor positivity. *J Nucl Med.* 2021;62:1082–1088.
45. Rauscher I, Krönke M, König M, et al. Matched-pair comparison of ^{68}Ga-PSMA-11 PET/CT and ^{18}F-PSMA-1007 PET/CT: frequency of pitfalls and detection efficacy in biochemical recurrence after radical prostatectomy. *J Nucl Med.* 2020;61:51–57.